JREE: Vol. 3, No. 1, (Winter 2016) 43-51

Journal of Renewable Energy and Environment

Research Article

Journal Homepage: www.jree.ir

Multi-objective Optimization of a Solar Driven Combined Power and Refrigeration System Using Two Evolutionary Algorithms Based on Exergoeconomic Concept

V. Sabeti[a]*, F. A. Boyaghchi[b]

[a]*Department of Computer Engineering, Alzahra University, Tehran, Iran*
[b]*Department of Mechanical Engineering, Alzahra University, Tehran, Iran*

PAPER INFO

Paper history:
Received 19 September 2015
Accepted in revised form 05 January 2016

Keywords:
Solar Energy
Cogeneration
Multi-Objective Optimization
NSGA-II
MOPSO

ABSTRACT

This paper deals with a multi-objective optimization of a novel micro solar driven combined power and ejector refrigeration system (CPER). The system combines an organic Rankine cycle (ORC) with an ejector refrigeration cycle to generate electricity and cold capacity simultaneously. Major thermodynamic parameters, namely turbine inlet temperature, turbine inlet pressure, turbine back pressure, and evaporator temperature are selected as the decision variables. Three objective functions, namely the energetic efficiency, exergetic efficiency and cost rate of products are selected for optimization. NSGA-II and MOPSO are employed and compared, to achieve the final solutions in the multi-objective optimization of the system operating. It is found that the values of the energetic and exergetic efficiencies increase within 27.7% and 26.1%, respectively and the cost rate of products decreases by about 32.7% with respect to base case.

1. INTRODUCTION

Low-grade heat sources, such as waste heat from industrial plants, geothermal resources and solar energy can be converted into various forms of energies.

In literature review, many works have been allocated on the combined power and absorption refrigeration cycle to employ the low temperature heat sources. Firstly, Goswami [1] proposed a novel cogeneration power and refrigeration cycle using ammonia-water mixture as the working fluid. Some further researchers [2-10] studied the proposed cycle by Goswami both theoretically and experimentally.

In Gaswami proposed cycle, refrigeration output was relatively small, because the ammonia-water phase does not change during the refrigeration process. In order to provide more refrigeration output, some novel combined power and absorption refrigeration cycle were proposed by other researchers.

Zheng et al. [11] proposed a modified cogeneration power and cooling cycle based on Kalina cycle. In this cycle, the flash tank was replaced by a rectifier for obtaining a higher concentration ammonia vapor for refrigeration. An evaporator and a condenser were applied between the rectifier and the second absorber. Zhang and Lior [12, 13] proposed several new combined power and ammonia-water absorption refrigeration cycle with both parallel and series connected configuration, they also studied the effect of the key thermodynamic parameters on both energy and exergy efficiencies. Liu and Zhang [14] proposed and analyzed a more advanced ammonia-water cycle to provide power and refrigeration upon the series connected configuration. They introduced a splitting/absorption in order to adjust some steam mass flow rates and maintain the desired ammonia concentrations in different processes. Wang et al. [15] proposed a simple combined power and refrigeration cycle based on Rankine and absorption refrigeration cycle. In this cycle the pump and condenser before and after the turbine are eliminated. The turbine exhaust with pressure which is higher than environment pressure can be condensed in the absorber. In this study, exergy efficiency of cycle is maximized by means of genetic algorithm. It is found that little attention has been paid to the cogeneration based on Rankine cycle and ejector refrigeration cycle.

*Corresponding Author's Email: vajiheh.sabeti@gmail.com (V. Sabeti)

Alexis [16] studied a combined power and ejector refrigeration cycle from view point of 1st law of thermodynamics. In this cycle, an extraction steam from steam turbine in conventional Rankine cycle evaporates the working fluid (water) in an independent steam ejector refrigeration cycle.

Dai et al. [17] proposed a new combined power and ejector refrigeration cycle using R123 as the working fluid for recovering low-grade heat effectively. In this cycle, a turbine is added between boiler and ejector to produce power and the turbine exhaust can drive the ejector to generate cooling in evaporator. They analyzed the desired cycle by applying 2nd law of thermodynamics. Wang et al. [18] proposed a new combined power and ejector refrigeration cycle which combines the Rankine cycle and the ejector refrigeration cycle by adding an extraction turbine between the ejector and the heat recovery vapor generator (HRVG). The vapor from the HRVG could be expanded through the turbine to produce power, and the turbine extraction vapor could drive the ejector to generate refrigeration simultaneously. Zheng and Weng [19] proposed a novel combined power and ejector refrigeration cycle based on the organic Rankine cycle (ORC) using various refrigerants. The ejector is driven by the exhausts from the turbine to produce power and refrigeration simultaneously. The proposed cycle had a big potential to produce refrigeration. Habibzadeh et al. [20] investigated the performance of the cycle proposed by Wang et al. [18] for several working fluids by applying 1st and 2nd law of thermodynamics. Also, they calculated the value of the thermal conductance of the heat exchangers. In addition, a parameter optimization is achieved by means of genetic algorithm to reach the maximum exergy efficiency.

This work proposes a novel CPER cycle based on ORC integrated with evacuated solar collector. The proposed cycle is simulated based on thermodynamic and thermoeconomic concept. A thermal storage tank is employed to store solar energy collected by collectors and supply energy to the CPER subsystem continuously even when the solar radiation is not sufficient. NSGA-II and MOPSO are employed to conduct the multi-objective optimization. The energetic efficiency, exergetic efficiency and cost rate of products are selected as the objective functions. Turbine inlet temperature, turbine inlet pressure, turbine back pressure and evaporator temperature are selected as the decision variables.

2. SYSTEM DESCRIPTION AND ASSUMPTIONS

Figure 1. illustrates the proposed CPER cycle. The main energy source of the whole system is evacuated by tube solar collector. The auxiliary boiler is installed as the backup energy source and it is used when the temperature of the thermal storage is lower than allowable temperature; on the other hand, thermal storage is used when solar radiation is insufficient.

The high pressure and temperature vapor generated by absorbing heat from solar energy is expanded through the turbine to generate power.

The extracted vapor of the turbine enters the supersonic nozzle of ejector. The very high velocity vapor at the exit of the nozzle produces a high vacuum at the inlet of the mixing chamber and entrains secondary vapor into the chamber from the evaporator. The two streams are mixed in the mixing chamber. Then the mixed stream becomes a transient supersonic stream. One entering the constant cross-section zone, a normal shock wave occurs, accompanied by a significant pressure rise. After the shock, the velocity of the mixed stream becomes subsonic and decelerates in the diffuser. The outlet stream from ejector is mixed with turbine outlet in mixer and discharged to the condenser to convert to liquid by rejecting heat to cooling water.

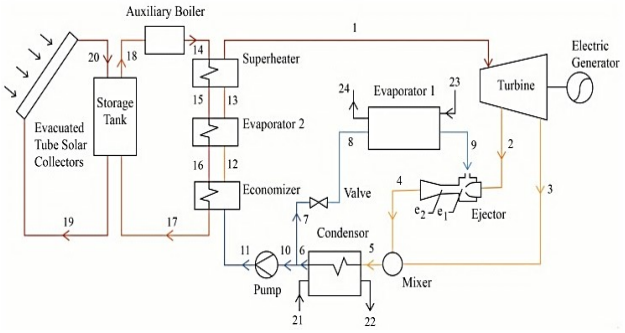

Figure 1. Schematic diagram of the Solar-Fuelled CPER System.

R123 is utilized as the working fluid because it is recognizable as a low pressure refrigerant that is nonflammable, nontoxic and non-corrosive. Thermodynamic modeling of the solar CPER system has been conducted based on simulation code in Engineering Equation Solver (EES) [21] . The main assumptions for the modeling of the combined cycle are listed in Table 1.

3. MATHEMATICAL MODEL

3.1. Thermodynamic analysis The thermodynamic modeling of the solar-fuelled CPER system mainly consists of the solar collection models and the CPER models. In order to simulate the CPER subsystem, the principles of mass and energy conservation are used. Neglecting the kinetic and potential energies, the general equations of these principles for a steady state process are specified below [22] :

$$\sum \dot{m}_i = \sum \dot{m}_e \tag{1}$$

$$\sum \dot{Q} - \sum \dot{W} = \sum \dot{m}_e h_e - \sum \dot{m}_i h_i \tag{2}$$

TABLE 1. Simulation conditions for the Solar-Fuelled CPER System.

ORC subsystem	
Turbine inlet pressure	1000 kPa
Turbine inlet temperature	130 °C
Ejector back pressure	91.48 kPa
mass flow extraction ratio	0.5
Turbine isentropic efficiency	0.85
Evaporation temperature	-5 °C
Pump isentropic efficiency	0.7
Cooling water inlet temperature	15 °C
Cooling water mass flow	0.4 kg/s
Cooling load	4.5 kW
Electrical generator efficiency	0.95
Pinch point temperature difference	5 °C
Cooling water inlet pressure	300 kPa
Dead state temperature	15 °C
Solar subsystem	
Monthly average insolation, $\bar{H}$	28.5 MJ/m^2.day
Monthly averaged insolation clearness index, $\bar{K}_T$	0.7
Tilt angle (°)	37.4
Optical efficiency η_0	0.656
Coefficient a_1	1.4 W/m.K
Coefficient a_2	0.007 W/m.K

where $\dot{m}$, $\dot{Q}$, $\dot{W}$ and h are mass flow rate, heat transfer rate, power and enthalpy, respectively and The subscripts i and e refer to input and output stream. Ejector is a major component in CPER subsystem and its performance is dependent upon entrainment ratio which determines the magnitude of mass flow rate of secondary refrigerant in terms of mass flow rate of primary refrigerant coming out from the turbine. Its model has been carried out based on the one-dimensional constant pressure model which is used by most researchers [23, 24]. It is known that the performance of ejector is evaluated by its entrainment ratio μ and given as:

$$\mu = \sqrt{\eta_n \eta_m \eta_{dif}\,(h_2 - h_{e1,s})/(h_{4,s} - h_{e2})} - 1 \quad (3)$$

where the efficiencies of nozzle, η_n, mixing and diffuser sections efficiencies η_m, η_{dif} are assumed to be 0.9, 0.85 and 0.85 respectively [23, 24] and subscript *s* refers to isentropic process. When the inlet state parameters of primary flow, secondary flow and back pressure of the ejector are given, the value of entrainment ratio μ could be found using iterative calculation.

The evacuated tube collector is selected to absorb the solar radiation. The hourly radiation falling on a tilted surface is obtained from the following relations [25]:

$$I_t = I_b R_b + I_d R_d + (I_b + I_d) R_R \quad (4)$$

where I_b and I_d are the hourly beam and diffuse radiation falling on collector surface, R_b, R_d, and R_R are defined as tilt factors for different radiations [25].

The solar radiation and the ambient temperature are assumed to be constant within one hour. The useful heat gained by solar collector, Q_u is calculated from the heat balance in the solar collector [25]:

$$Q_u = \eta_{Coll} \times A_{Coll} \times I_t \quad (5)$$

η_{Coll} is defined as the ratio of the useful heat gain to the incident solar radiation and A_{coll} stands for evacuated tube solar collectors area. Solar collector efficiency can be calculated using the following thermal performance equations [26]:

$$\eta_{Coll} = \eta_o - \left(\frac{T_a - T_0}{I_t}\right) \times a_1 - \left(\frac{(T_a - T_0)^2}{I_t}\right) \times a_2 \quad (6)$$

where η_o, T_a and T_0 are collector optical efficiency, ambient temperature and dead state temperature, respectively and a_2 and a_2 are the heat loss coefficient and adopted from product specification sheet of the selected collector [27].

A thermal storage tank is installed to act as a buffer between the solar collector and the CPER subsystems. The storage tank is assumed to be insulated and the water is assumed to be completely mixed so that the water temperature T varies only with time. The following equation can be obtained from the energy balance in the tank [28]:

$$\left[(\rho V C_P)_W + (\rho V C_P)_{\tan k}\right]\frac{dT}{dt} = Q_u - Q_{load} - (UA)_{\tan k}.(T - T_a) \quad (7)$$

where $(\rho VC_P)_W$ refers to the heat capacity of the water in the tank, $(\rho VC_P)_{tank}$, the heat capacity of the tank material (steel in this study), T_a, the ambient temperature around the tank, and $(UA)_{tank}$, the product of the overall heat transfer coefficient and surface area of the tank. Q_u and Q_{load}, represent the useful gain from the solar collectors and energy discharged to CPER subsystem and can be calculated as**:**

$$Q_{load} = (mC_P)_W (T - T_{17}) \quad (8)$$

Due to thermodynamic irreversibility, the exergy analysis is required to evaluate in each components. By identifying 'fuel–product–loss' (F–P–L) exergy for each component of the system, the exergy destruction in each component is calculated as follows [29]:

$$\dot{X}_D = \dot{X}_F - \dot{X}_P - \dot{X}_L \quad (9)$$

where $\dot{X}$ refers to total physical exergy steam in each point.

3.2. Economic model A cost balance applied to each component shows that the sum of cost rates associated with all exiting exergy streams equals the sum of cost rates of all entering exergy streams plus the appropriate charges due to capital investment $\dot{Z}^{CI}$ and

operating and maintenance expenses $\dot{Z}^{OM}$ the sum of the last two terms is denoted by $\dot{Z}$. Accordingly, using the cost rate associated with fuel, product, and exergy loss for each component, the cost rate balance can be written as follows[29]:

$$\dot{C}_P = \dot{C}_F - \dot{C}_L + \dot{Z} \tag{10}$$

where $\dot{C}$ represents cost rate and subscripts P, F and L refer to product, fuel and loss for each component, respectively. Since the solar energy is cost free, only the cost of each component is considered in economical modeling. The cost working fluid, piping and labour is also not considered in economic modeling. Considering the super heater, evaporator, economizer and heater as heat exchangers, the capital cost of the system components can be listed in Table 2. in which A_{HE} and V_{ST} stand for the heat exchanger area and storage tank volume, repectively.

Also, capital investments of solar collector and auxiliary boiler in the reference year (2013) is 567 \$/m^2 and 28 \$/kW [30]. It should be noted that capital investments of ejector, mixers and valves are neglected in the analysis because of being much lower than other components.

Capital investment of a component is converted to the cost rate by multiplying it by 1/t, the capital recovery factor (CRF) and maintenance factor (φ). Here, t is the number of hours per year that the unit operates and the CRF is an economic parameter that depends on the interest rate (i) and the estimated component lifetime (N). The CRF is determined as follows [31]:

$$CRF = \frac{i(1+i)^N}{(1+i)^N - 1} \tag{11}$$

In the above components, investment cost rate is calculated by following equation [32]:

$$\dot{Z} = Z^{CI} \times CRF \times \varphi / t \tag{12}$$

where N, i, φ and t are taken as 20 year, 10%, 1.06 and 7446h, respectively.

TABLE 2. The capital cost relation for each component of desired system.

Components	Capital cost relation
Heat exchanger [32]	$Z_{HE}^{CI} = 130\left(\frac{A_{HE}}{0.093}\right)^{0.78}\ [0,1]$
Condenser [32]	$Z_{Cond}^{CI} = 1773\,\dot{m}_5$
Pump [32]	$Z_{pump}^{CI} = 3540\ \dot{W}_{pump}^{0.71}$
Storage tank [33]	$Z_{ST}^{CI} = 4042\ V_{ST}^{0.506}$
Turbine [34]	$\log_{10}(Z_{Turb}^{CI}) = 2.6259 + 1.4398\ \log_{10}(\dot{W}_{Turb}) - 0.1776\left[\log_{10}(\dot{W}_{Turb})\right]^2$
Electric generator [35]	$Z_{Elec}^{CI} = 60\ \dot{W}_{Elec}^{0.95}$

3.3. Performance criteria In order to evaluate the system performance from both thermodynamic and economic aspects, the energetic efficiency (η_{en}), exergetic efficiency (η_{ex}) and cost rate of products ($\dot{C}_{P,tot}$) are defined as follows:

$$\eta_{en} = \frac{\dot{W}_{Elec} + \dot{Q}_{Evap1}}{A_{Coll} \cdot I_t + \dot{m}_{NG} \cdot LHV_{NG}} \tag{13}$$

where, $\dot{W}_{Elec}$ stands for electrical power, $\dot{Q}_{Evap1}$, cooling process, $\dot{m}_{NG}$, mass flow rate of natural gas, and LHV, Lower heating value of natural gas taken as 50654 kJ/kg[29].

$$\eta_{ex} = \frac{\dot{W}_{Elec} + \dot{X}_{Eva1}}{\dot{X}_{sun} + \dot{X}_{NG}} \tag{14}$$

In Eq.(14) $\dot{X}_{Eva1}$ represents the exergy rate of cooling process in evaporator1 and the exergy of sun $\dot{X}_{sun}$ can be determined by following [36-38]:

$$\dot{X}_{sun} = I_t A_{Coll}\left[1 + \frac{1}{3}\left(\frac{T_o}{T_{sun}}\right)^4 - \frac{4}{3}\left(\frac{T_o}{T_{sun}}\right)\right] \tag{15}$$

where, specific exergy of natural gas is 51393 kJ/kg [29] and the temperature of sun (T_s) is taken as 6000 K [25].

$$\dot{C}_{P,tot} = \dot{C}_{P,Elec} + \dot{C}_{P,Evap1} \tag{16}$$

In which, cost rate of overall system consists of electricity load produced by generator and cooling load generated by evaporator 1.

3.4. Results and discussion In order to achieve the optimal performance of the solar-fuelled CPER system, we conduct the optimization using NSGA-II and MOPSO. Four key thermodynamic parameters, namely turbine inlet temperature, turbine inlet pressure, turbine back pressure and evaporator temperature are chosen as the decision variables. The merit of multi objective optimization of energetic efficiency, exergetic efficiency and product cost rate is to achieve the optimum effectiveness of cycle. The ranges of the decision variables in the optimization are listed in Table 3. Table 4. indicates the control parameters in NSGA-II method.

TABLE 3. Decision variables and their lower and upper boundaries.

Variables	Lower bound	Upper bound
Turbine inlet temperature/°C	130	145
Turbine inlet pressure/kPa	1000	1400
Turbine back pressure/kPa	200	300
Evaporator temperature/ °C	-5	0

Since the optimization consists of three various objective functions, the solution space is three dimensions (3D). In this case, to illustrate the Pareto

front obtained from optimization algorithm, a 3D figure is required. In order to clarify the outcomes in 3D figure, three 2D figures can be drawn including two objective functions. Figure 2. demonstrates the 3D Pareto frontier solutions for the solar -fuelled CPER system of multi-objective optimization based on NSGA-II, and Figures 3-5. show the projects of 3D Pareto Frontier on each plate of coordinate which reveal the conflicts between efficiencies and cost rate of products. The comparison of the four figures indicates that the energetic efficiency remains constant versus exergetic efficiency and cost rate of total products.

TABLE 4. Control parameters in NSGA-II.

Parameters	value
Population size	50
Crossover probability	0.7
Mutation probability	0.4
Maximum generation	50

In these figures, each point located on the Pareto frontier is potentially an optimum solution. A larger value of exergetic efficiency can be obtained by reducing the exergy destruction and loss of overall system which leads to increment of total capital investment cost rate. Therefore, the maximum exergy efficiency defined as design point A leads to the maximum value of the cost rate of total products as well.

The minimum value of exergetic efficiency is defined as design point B, with corresponding minimum value of cost rate of products. Design points of A and B respectively refer to the optimum solutions of single-objective function where the cost rate of products or the exergetic efficiency is selected as the objective function. Since it is impossible to make each objective at its optimum value simultaneously, the absolute optimum solution of multi-objective does not exist. The point satisfying the result with the minimum total heat transfer and the maximum average useful output simultaneously does not exist in the optimal solutions, shown as Point D in Figure 3. Therefore, in this paper, the point which is the closest point to the specific point D, is decided to be the final solution in the multi-objective optimization. Thus, to achieve the final solution, a process of decision-making is required with the aid of a hypothetical point D[39] which is the intersection of minimum cost rate of products and maximum exergetic efficiency and is not located on the Pareto Frontier. In this study, the closest point C of the Pareto Frontier to the hypothetical point D is considered as the final solution. At point C, the system achieves the best possible values considering two objective functions.

Table 5. lists the optimum objective function values and the corresponding decision variables for points A–C on the Pareto frontier and the corresponding detailed parameter distribution on the system based on NSGA-II.

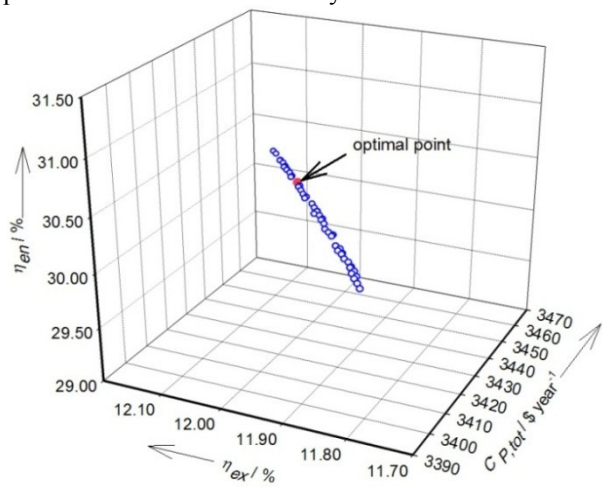

Figure 2. Pareto frontier for cost rate of products versus energetic and exergetic efficiencies using NSGA-II.

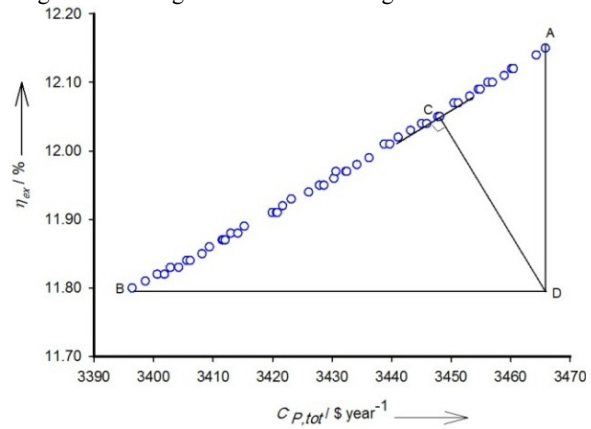

Figure 3. Pareto frontier for cost rate of products versus exergetic efficiency using NSGA-II.

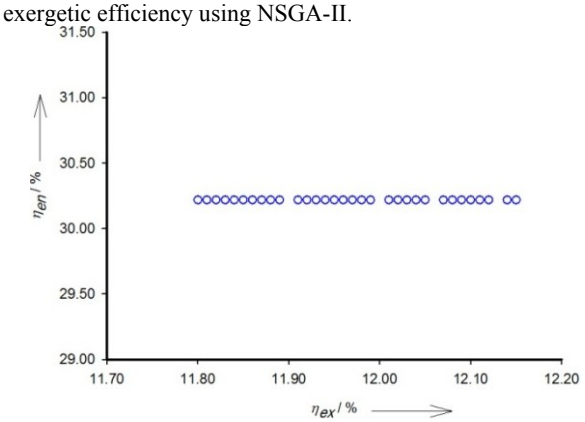

Figure 4. Pareto frontier for versus exergetic efficiency versus energetic efficiency using NSGA-II.

Results indicate that under the condition of the optimum solutions of the single and multi-objective optimization the values of turbine inlet temperature and turbine inlet pressure are close to their maximum ranges while the value of turbine back pressure is located close to minimum value of its range.

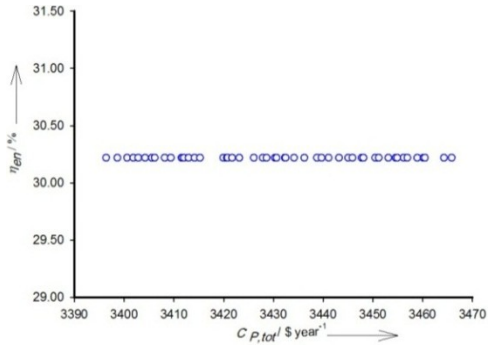

Figure 5. Pareto frontier for cost rate of products versus energetic efficiency using NSGA-II.

TABLE 5. Optimum values of objective and decision variables for points A–C on the Pareto optimal front using NSGA-II.

Point	A	B	C
Turbine inlet temperature/^{o}C	145	145	144.97
Turbine inlet pressure/kPa	1400	1400	1399.96
Turbine back pressure/kPa	200.04	200	200.01
Condensation temperature/^{o}C	-5	0	-3.1591
Cost rate of products ($\dot{C}_{P,tot}$)	3465	3396	3441
Energetic efficiency (η_{en})	30.22	30.22	30.22
Exergetic efficiency (η_{ex})	12.15	11.79	12.01

Multi-objective particle swarm optimization (MOPSO) is applied for comparing the values of optimum points obtained with NSGA-II method. Table 6. indicates the Control parameters in MOPSO used for optimization.

TABLE 6. Control parameters in MOPSO.

Parameters	value
Population size	50
Repository size	50
Inertia Weight	0.7
Personal Learning Coefficient	1
Global Learning Coefficient	2
Number of Grids per Dimension	5
Mutation probability	0.1
Maximum generation	50

Figures (6-9). demonestrates the Pareto frontier solutions for the solar -fuelled CPER system of multi-objective optimization based on MOPSO. The results discussion in this method is the same as NSGA-II. Table 7. shows the values of the constraints and multi-objective optimization of overall system performance for each point of A, B and C using the MOPSO method. Since the value of energetic efficiency for each point located in Pareto frontier is fixed, identifying the points A, B, C and D in NSGA-II and MOPSO are performed using Figures 3. and 7. respectively. The comparison of results obtained from NSGA-II and MOPSO indicates that in point A the value of energetic efficiency is dominant and its values determined from NSGA-II and MOPSO are 12.15% and 12.12%, respectively which shows the optimal condition in NSGA-II method. In point B the value of the cost rate of products is minimum. The values determined from NSGA-II and MOPSO are 3396 and 3421 $/year, respectively. Therefore, NSGA-II leads to optimal value. In point C, this point is the optimal point in multi-objective optimization in which the value of cost rate of products is minimum and the value of exergetic efficiency is maximum. The compassion between both methods indicates the same values for C. Therefore, if the purpose is identifying the point C, each method can be selected for optimization.

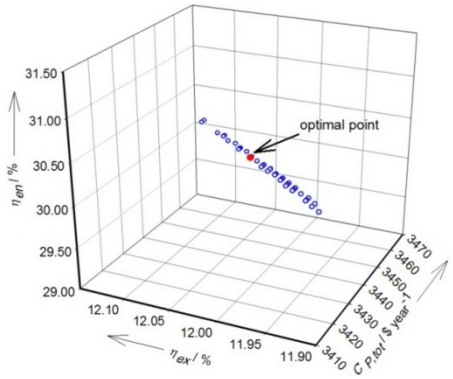

Figure 6. Pareto frontier for cost rate of products versus exergetic efficiency versus energetic efficiency using MOPSO.

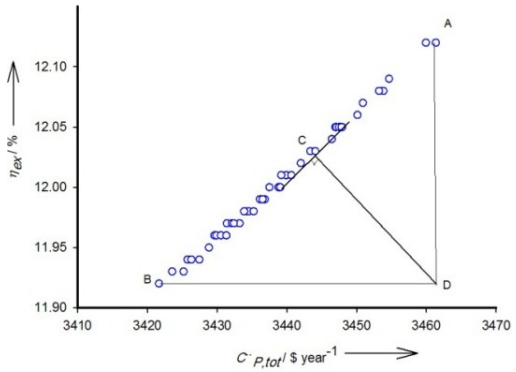

Figure 7. Pareto frontier for cost rate of products versus exergetic efficiency using MOPSO.

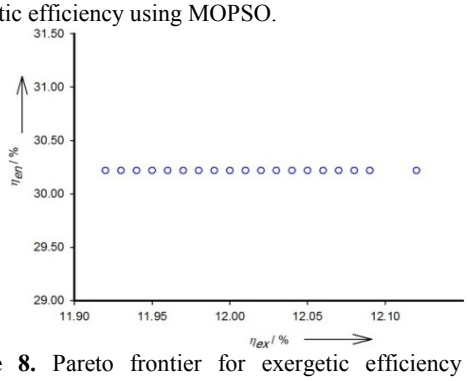

Figure 8. Pareto frontier for exergetic efficiency versus energetic efficiency using MOPSO.

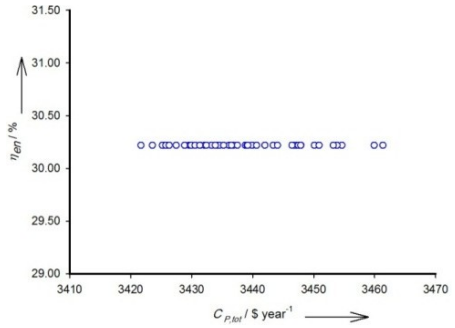

Figure 9. Pareto frontier for cost rate of products versus energetic efficiency using MOPSO.

TABLE 7. Optimum values of objective and decision variables for points A–C on the Pareto optimal front using MOPSO.

Point	A	B	C
Turbine inlet temperature/^{o}C	145	144.9934	144.94
Turbine inlet pressure/kPa	1400	1400	1399.96
Turbine back pressure/kPa	200	200	200.05
Condensation temperature/^{o}C	-4.6665	-1.76688	-3.30
Cost rate of products ($\dot{C}_{P,tot}$)	3461	3421	3443
Energetic efficiency (η_{en})	30.22	30.22	30.22
Exergetic efficiency (η_{ex})	12.12	11.92	12.02

One approach for optimization of the mentioned objective functions is the single objective optimization. According to the conflicts among the objective functions the thermodynamic properties obtained from optimizing of one objective function cannot lead to optimization of the other objective functions. This subject can be confirmed by results listed in Table 8. This Table indicates the results obtained by the single objective optimization of each η_{en}, η_{ex} and $\dot{C}_{P,tot}$. Points A and B are obtained by multi-objective optimization based on NSGA-II. These points represent the maximum energetic efficiency and the minimum cost rate of products, respectively. As it is obvious, the values of energetic efficiency in point A and cost rate of products in point B obtained from NSGA-II are as same as the results obtained from the single objective optimization. Also, it is found that the value of energetic efficiency obtained from the single and multi-objective optimization is 30.22%.

The comparison between multi-objective optimization and the base case results, shows that in NSGA-II method, the energetic efficiency increases from 23.66% to 30.22%, the exergetic efficiency increases within 26.2% and the cost rate of products decreases 32.72%. In MOPSO method, the energetic efficiency increases from 23.66% to 30.22%, the exergetic efficiency increases within 27.70% and the cost rate of products decreases within 32.68%.

According to Figures 4, 5, 8, 9. and Tables 7. and 8. it seems that optimization procedure does not influence the energetic effieincy because all points on Pareto front show a value for energetic efficiency but if this value is compared with the base one, it is clearly observed that energetic efficiency as an objective function improves relative to the base case. The intresting point is that the values of energetic efficiencies on Pareto front are exactly equal to the value of energetic efficiency in single objective optimization which is the ideal case and does not obtained in the most cases, i.e. the equality of the objective functions in optimum point for multi and single objective cases.

TABLE 8. Comparison of optimization results between single-objective and multi-objective (NSGA-II).

Term	Base case	Multi-objective (B point)	Single-objective ($\dot{C}_{P,tot}$)	Multi-objective (A point)	Single-objective (η_{ex})	Single-objective (η_{en})
$\dot{C}_{P,tot}$	5115	3396	3396	3465	3466	3411
η_{ex}	9.51	11.79	11.79	12.15	12.15	11.86
η_{en}	23.66	30.22	30.22	30.22	30.22	30.22

Finally, it should be mentioned that the performance and ability of each multi objective optimization algorithm differs from others. The present outcomes indicate that Pareto front obtained from MOPSO and NSGA-II algorithms are not completely similar. In addition, their optimal pointss differ. The high convergence velocity and the simplicity of MOPSO algorithm are the advantages of this algorithm relative to NSGA-II while its Pareto front covers less space than NSGA-II one [40-42]. Therefore, if obtaining points A and B to be our objective, NSGA-II leads to the better solution while the optimal points calculated from the both algorithms are almost the same.

4. CONCLUSIONS

This paper has presented a micro solar cogeneration cycle for generating power and refrigeration simultaneously. Evolutionary algorithms are utilized for multi-objective optimization of the overall system performance. Some remarks can be concluded from this research as follows:

- The results of the closest point (C) of Pareto Frontier to the hypothetic point (D) are approximately the same in both NSGA-II and MOPSO methods. In this point the energetic efficiency and exergetic efficiency increase within 27.7% and 26.1% respectively and the cost rate of products decreases 32.7% in comparison with base case.
- Although the point C is not an ideal point, the value of energetic efficiency in this point (30.22%) is the same as its value determined from the single objective optimization.

- The corresponding values of point A and B determined from NSGA-II method are better than those obtained from MOPSO method.

Nomenclature

A	Surface area of solar collector (m^2)
$\dot{C}$	Coast rate ($/year)
C_p	Specific heat (kJ/kg K)
H	Monthly average radiation (J/m^2 day)
h	Specific enthalpy (kJ/ kg)
i	Interest rate (%)
K_T	Monthly average clearness index
LHV	Lower heating value (kJ)
$\dot{m}$	Mass flow rate (kg/s)
$\dot{Q}$	Heat rate (kW)
R	Tilt factor
t	System operating hours (hour)
T	Temperature (^oC or K)
V	Volume (m^3)
$\dot{W}$	Power (kW)
$\dot{X}$	Exergy rate (kW)
Z	Investment cost ($)
$\dot{Z}$	Investment cost rate ($/year)

Subscripts

0	Dead state
a	Ambient
b	Beam
Coll	Solar collector
Cond	Condenser
D	Destruction
d	Diffuse
dif	Ejector diffuser
e	Exit
Elec	Electric generator
en	Energy
Eva	Evaporator
ex	Exergy
F	Fuel
HE	Heat exchanger
i	Inlet
is	Isentropic
L	Loss
LHV	Lower Heating Value (kJ/kg)
m	Ejector mixer
n	Ejector nozzle
NG	Natural gas
P	Product
pump	Pump
SH	Super heater
ST	Storage tank
sun	sun
t	Tilt
tank	Tank
Turb	Turbine
u	Useful
w	water

Super scripts

CI	Capital Investment
N	component lifetime (year)
OM	operating and maintenance

Greek symbols

η	Thermal efficiency (%)
μ	Entrainment ratio
ε	Exergy efficiency
φ	Maintenance factor

Abbreviation

CPER	Combined Power and Ejector Refrigeration
CRF	Capital Recovery Factor
ORC	Organic Rankine Cycle

REFERENCES

1. Goswami, D., "Solar thermal power: status of technologies and opportunities for research", ***Heat and Mass Transfer,*** Vol. 95, (1995), 57-60.
2. Goswami, D.Y. and Xu, F., "Analysis of a new thermodynamic cycle for combined power and cooling using low and mid temperature solar collectors", ***Journal of Solar Energy Engineering,*** Vol. 121, No. 2, (1999), 91-97.
3. Xu, F., Goswami, D.Y. and Bhagwat, S.S., "A combined power/cooling cycle", ***Energy,*** Vol. 25, No. 3, (2000), 233-246.
4. Hasan, A.A., Goswami, D.Y. and Vijayaraghavan, S., "First and second law analysis of a new power and refrigeration thermodynamic cycle using a solar heat source", ***Solar Energy,*** Vol. 73, No. 5, (2002), 385-393.
5. Goswami, D.Y., Vijayaraghavan, S., Lu, S. and Tamm, G., "New and emerging developments in solar energy", ***Solar Energy,*** Vol. 76, No. 1, (2004), 33-43.
6. Tamm, G., Goswami, D.Y., Lu, S. and Hasan, A.A., "Theoretical and experimental investigation of an ammonia–water power and refrigeration thermodynamic cycle", ***Solar Energy,*** Vol. 76, (2004), 217-228.
7. Vidal, A., Best, R., Rivero, R. and Cervantes, J., "Analysis of a combined power and refrigeration cycle by the exergy method", ***Energy,*** Vol. 31, No. 15, (2006), 3401-3414.
8. Vijayaraghavan, S. and Goswami, D.Y., "A combined power and cooling cycle modified to improve resource utilization efficiency using a distillation stage", ***Energy,*** Vol. 31, (2006), 1177-1196.
9. Martin, C. and Goswami, D.Y., "Effectiveness of cooling production with a combined power and cooling thermodynamic cycle", ***Applied Thermal Engineering,*** Vol. 26, (2006), 576-582.
10. Sadrameli, S. and Goswami, D.Y., "Optimum operating conditions for a combined power and cooling thermodynamic cycle", ***Applied Energy,*** Vol. 84, No. 3, (2007), 254-265.
11. Zheng, D., Chen, B., Qi, Y. and Jin, H., "Thermodynamic analysis of a novel absorption power/cooling combined-cycle", ***Applied Energy,*** Vol. 83, No. 4, (2006), 311-323.
12. Zhang, N. and Lior, N., "Development of a novel combined absorption cycle for power generation and refrigeration", ***Journal of Energy Resources Technology,*** Vol. 129, No. 3, (2007), 254-265.

13. Zhang, N. and Lior, N., "Methodology for thermal design of novel combined refrigeration/power binary fluid systems", ***International Journal of Refrigeration,*** Vol. 30, No. 6, (2007), 1072-1085.
14. Liu, M. and Zhang, N., "Proposal and analysis of a novel ammonia–water cycle for power and refrigeration cogeneration", ***Energy,*** Vol. 32, No. 6, (2007), 961-970.
15. Wang, J., Dai, Y. and Gao, L., "Parametric analysis and optimization for a combined power and refrigeration cycle", ***Applied Energy,*** Vol. 85, No. 11, (2008), 1071-1085.
16. Alexis, G.K., "Performance parameters for the design of a combined refrigeration and electrical power cogeneration system", ***International Journal of Refrigeration,*** Vol. 30, No. 6, (2007), 1097-1103.
17. Dai, Y., Wang, J. and Gao, L., "Exergy analysis, parametric analysis and optimization for a novel combined power and ejector refrigeration cycle", ***Applied Thermal Engineering,*** Vol. 29, No. 10, (2009), 1983-1990.
18. Wang, J., Dai, Y. and Sun, Z., "A theoretical study on a novel combined power and ejector refrigeration cycle", ***International Journal of Refrigeration,*** Vol. 32, No. 6, (2009), 1186-1194.
19. Zheng, B. and Weng, Y.W., "A combined power and ejector refrigeration cycle for low temperature heat sources", ***Solar Energy,*** Vol. 84, No. 5, (2010), 784-791.
20. Habibzadeh, A., Rashidi, M.M. and Galanis, N., "Analysis of a combined power and ejector-refrigeration cycle using low temperature heat", ***Energy Conversion and Management,*** Vol. 65, (2013), 381-391.
21. http://www.fchart.com. Engineering Equation Solver (EES).
22. Cengel, A.Y. and Boles, M.A., "Thermodynamics: An engineering approach", New York: McGraw Hill, (2008).
23. Ouzzane, M. and Aidoun, Z., "Model development and numerical procedure for detailed ejector analysis and design", ***Applied Thermal Engineering,*** Vol. 23, No. 18, (2003), 2337-2351.
24. Huang, B.J., Chang, J.M., Wang, C.P. and Petrenko, V.A., "A 1-D analysis of ejector performance", ***International Journal of Refrigeration,*** Vol. 22, No. 5, (1999), 354-364.
25. kalogirou, s., "solar energy engineering: processes and systems", UK: Elsevier, (2009).
26. Zhang, W., Ma, X., Omer, S.A. and Riffat, S.B., "Optimum selection of solar collectors for a solar-driven ejector air conditioning system by experimental and simulation study", ***Energy Conversion and Management,*** Vol. 63, No. 0, (2012), 106-111.
27. http://www.apricus.com.au/downloads/. Apricus Collector Specifications.
28. Sukhatme, K. and Sukhatme, S.P., "Solar energy: principles of thermal collection and storage", Tata McGraw-Hill Education, (1996).
29. Bejan, A. and Moran, M.J., "Thermal design and optimization", Wiley. com, (1996).
30. http://www.apricus.com.au/downloads/. product specification sheet.
31. Garousi Farshi, L., Mahmoudi, S.M.S. and Rosen, M.A., "Exergoeconomic comparison of double effect and combined ejector-double effect absorption refrigeration systems", ***Applied Energy,*** Vol. 103, (2013), 700-711.
32. Mohammadkhani, F., Shokati, N., Mahmoudi, S.M.S., Yari, M. and Rosenc, M.A., "Exergoeconomic assessment and parametric study of a Gas Turbine-Modular Helium Reactor combined with two Organic Rankine Cycles", ***Energy,*** Vol. 65, (2014), 533-543.
33. Martínez-Lera, S., Ballester, J. and Martínez-Lera, J., "Analysis and sizing of thermal energy storage in combined heating, cooling and power plants for buildings", ***Applied Energy,*** Vol. 106, (2013), 127-142.
34. El-Emam, R.S. and Dincer, I., "Exergy and exergoeconomic analyses and optimization of geothermal organic Rankine cycle", ***Applied Thermal Engineering,*** Vol. 59, No. 1, (2013), 435-444.
35. Pierobon, L., Nguyen, T.V., Larsen, U., Haglind, F. and Elmegaard, B., "Multi-objective optimization of organic Rankine cycles for waste heat recovery: Application in an offshore platform", ***Energy,*** Vol. 58, (2013), 538-549.
36. Petela, R., "Exergy of undiluted thermal radiation", Solar ***Energy,*** Vol. 74, No. 6, (2003), 469-488.
37. Wall, G., Exergetics. See also: http://exergy. se. 1998, Mölndal, Sweden.
38. Zamfirescu, C. and Dincer, I., "How much exergy one can obtain from incident solar radiation?", ***Journal of Applied Physics,*** Vol. 105, No. 4, (2009).
39. Wang, M., Wang, J., Zhao, P. and Dai, Y., "Multi-objective optimization of a combined cooling, heating and power system driven by solar energy", ***Energy Conversion and Management,*** Vol. 89, (2015), 289-297.
40. Li, X. "A non-dominated sorting particle swarm optimizer for multiobjective optimization", ***Genetic and Evolutionary Computation—GECCO,*** Vol. 2723, (2003), 37-48.
41. Parsopoulos, K.E. and Vrahatis, M.N., "Particle swarm optimization method in multiobjective problems", ***Proceedings of the 2002 ACM symposium on Applied computing,*** (2002), 603-607.
42. Coello, C.A.C., Pulido, G.T. and Lechuga, M.S., "Handling multiple objectives with particle swarm optimization", ***Evolutionary Computation, IEEE Transactions,*** Vol. 8, No. 3, (2004), 256-279.